ACS APPLIED MATERIALS & INTERFACES

Research Article

www.acsami.org

Clean Method for the Synthesis of Reduced Graphene Oxide-Supported PtPd Alloys with High Electrocatalytic Activity for Ethanol Oxidation in Alkaline Medium

Fangfang Ren,[†] Huiwen Wang,[†] Chunyang Zhai,[†] Mingshan Zhu,[§] Ruirui Yue,[†,‡] Yukou Du,*[,†] Ping Yang,[†] Jingkun Xu,*[,‡] and Wensheng Lu*[,§]

[†]College of Chemistry, Chemical Engineering and Materials Science, Soochow University, Suzhou 215123, P. R. China

[‡]Jiangxi Key Laboratory of Organic Chemistry, Jiangxi Science and Technology Normal University, Nanchang 330013, P. R. China

[§]CAS Key Laboratory of Colloid, Interface and Chemical Thermodynamics, Institute of Chemistry, Chinese Academy of Sciences, Beijing 100190, China

Supporting Information

ABSTRACT: In this article, a clean method for the synthesis of PtPd/reduced graphene oxide (RGO) catalysts with different Pt/Pd ratios is reported in which no additional components such as external energy (e.g., high temperature or high pressure), surfactants, or stabilizing agents are required. The obtained catalysts were characterized by X-ray diffraction (XRD), transmission electron microscopy (TEM), high-resolution transmission electron microscopy (HRTEM), Raman spectroscopy, X-ray photoelectron spectroscopy (XPS), induced coupled plasma atomic emission spectroscopy (ICP–AES), and electrochemical measurements. The HRTEM measurements showed that all of the metallic nanoparticles (NPs) exhibited well-defined crystalline structures. The composition of these Pt–Pd/RGO catalysts can be easily controlled by adjusting the molar ratio of the Pt and Pd precursors. Both cyclic voltammetry (CV) and chronoamperometry (CA) results demonstrate that bimetallic PtPd catalysts have superior catalytic activity for the ethanol oxidation reaction compared to the monometallic Pt or Pd catalyst, with the best performance found with the PtPd (1:3)/RGO catalyst. The present study may open a new approach for the synthesis of PtPd alloy catalysts, which is expected to have promising applications in fuel cells.

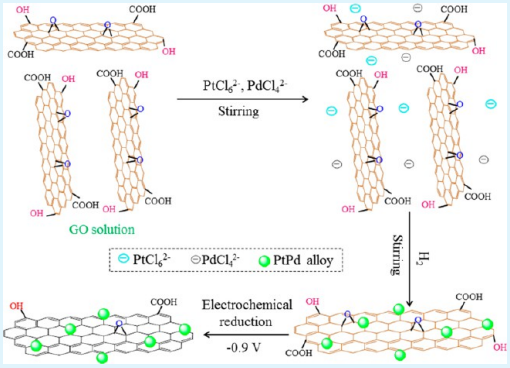

KEYWORDS: *PtPd nanoparticles, reduced graphene oxide, electrocatalytic activity, alkaline, fuel cell, ethanol oxidation*

1. INTRODUCTION

With the world's growing demand for energy coupled with concerns over environmental pollution and the rapid depletion of conventional energy sources, fuel cells have been receiving considerable attention because they are able to convert the chemical energy of combustion of small-molecule fuels directly into electricity.[1−3] Among the various liquid fuels, ethanol is an almost ideal fuel because of its low toxicity, high energy density (8 kWh kg^{-1}), and ability to be easily produced in large quantities via the fermentation of biomass.[4] For these reasons, the direct ethanol fuel cell (DEFC) has recently attracted much interest as a renewable power source for both portable and stationary electronic applications. To date, extensive research on DEFCs has been done under acidic conditions, and significant progress has been made in their development.[5,6] However, the slow reaction kinetics of ethanol oxidation in acidic media and the high loading of noble-metal catalysts are the main barriers to the commercialization of DEFCs.[7] It has been reported that the ethanol oxidation kinetics could be significantly improved by operating the DEFC in alkaline medium.[8] Moreover, pioneering works have shown that alloys of Pt with a second metal (such as Bi, Sn, Ru, Ni, and Pd) can not only accelerate ethanol oxidation but also reduce the Pt loading as well as improve the CO resistance of Pt, which has been explained by a bifunctional mechanism or an electronic effect between the two metals.[9−13] Among these elements, Pd is known to be a very good electrocatalyst for ethanol oxidation in alkaline media.[14,15] More importantly, Pd has very similar properties to Pt and is less expensive compared to Pt. Additionally, Pd is able to form alloys with Pt at all compositions.[16] Therefore, the combination of Pt with Pd could be expected to display better catalytic activity towards ethanol oxidation in alkaline media.

To maximize further the electroactivity of the catalysts and to minimize the usage of noble metals, loading the catalysts on the surface of a suitable supporting material that has a low cost,

Received: December 19, 2013
Accepted: January 23, 2014
Published: January 23, 2014

Scheme 1. Typical Procedure for the Synthesis of the PtPd/RGO Catalyst

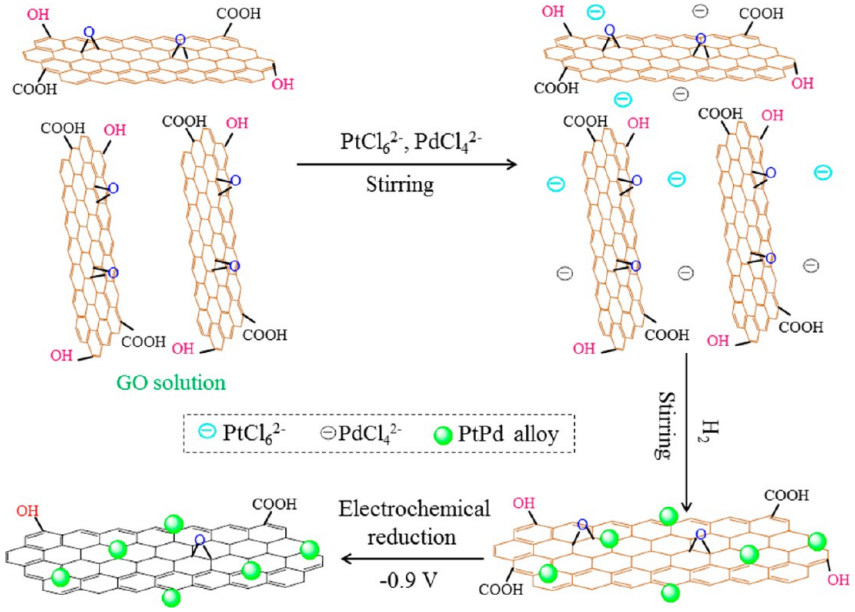

good conductivity, and high surface area is highly desirable.[17−21] Recently, graphene, a two-dimensional carbon material made up of a single or a few atomic layers, has received significant attention owing to its extremely high specific surface area (2630 m^2 g^{-1}), exceptional electrical conductivity (10^3 to 10^4 S m^{-1}), and superior thermal/chemical stability,[22−24] which makes it a promising catalyst support for fuel-cell applications. For instance, Guo et al.[22] developed a facile wet-chemical approach for the synthesis of high-quality three-dimensional (3D) Pt-on-Pd bimetallic nanodendrites supported on graphene sheets and found that the prepared graphene/bimetallic nanodendrite hybrids exhibited much higher electrocatalytic activity toward the methanol oxidation reaction than the platinum black (PB) and commercial E-TEK Pt/C catalysts. With the use of ethylene glycol (EG) as a reducing agent, Wen and co-workers[25] synthesized a Pd/SnO_2−graphene catalyst by a microwave-assisted reduction process, which displayed superior electrocatalytic activity for ethanol oxidation. However, it should be noted that all of these methods either used hydrazine or sodium borohydride as the reducing agent, which are highly toxic and may cause serious health or environmental problems, thus limiting their practical uses in a general case. Furthermore, some stabilizers such as octadecylamine or poly-vinylpyrrolidone (PVP) are usually introduced to anchor the metal NPs to the graphene surface and to stabilize metal NPs.[23,26] Nevertheless, the presence of these stabilizers could strongly absorb on the surface of metal NPs surface and then severely affect the electrocatalytic performance of the catalysts. In addition, the complete removal of these stabilizers without altering the NPs structure still remains a challenge.[27−29] Therefore, it is meaningful to develop an environmentally friendly and surfactant-free approach for the synthesis of metal/graphene nanocomposites that can overcome these two above-mentioned problems at the same time.

Herein, we report a novel and eco-friendly route to fabricate PtPd alloy NPs on RGO by a two-step reduction method, which is illustrated in Scheme 1. In the first step, $PtCl_6^{2-}$ and $PdCl_4^{2-}$ ions are completely reduced and deposited on sheets of graphite oxide (GO) using H_2 as the reducing agent, whereas GO is not reduced; thus, abundant functional groups on the surfaces of GO can be used as anchoring sites for metal NPs. The product obtained from this process is denoted as PtPd/GO. In the next step, GO is reduced by an electrochemical reduction method. Several benefits of this work are inspiring: (i) H_2 is a very clean reducing agent, and no residual chemical is left after the reduction process; (ii) this method yields small metal NPs with average diameters of ∼4−7 nm, which are evenly distributed on the GO surface; (iii) the as-prepared PtPd/GO formed a stable suspension for several months without any stabilizers or surfactants, and the surfactant-removal process at high temperatures can be avoided; and (iv) the PtPd/RGO catalyst exhibits higher electrocatalytic performance and stability toward ethanol oxidation in alkaline medium.

2. EXPERIMENTAL SECTION

2.1. Materials. In the present work, the preliminary materials are graphite powder (Sinopharm Chemicals Reagent Co., Ltd, China), $H_2PtCl_6{\cdot}6H_2O$ and H_2PdCl_4 (Shanghai Shiyi Chemicals Regent Co., Ltd, China), $NaNO_3$, $KMnO_4$, H_2O_2 (30%), CH_3CH_2OH, KOH, and H_2SO_4 (95%). All chemicals were of analytical grade and were used as received without any further purification. Phosphate buffer solution (PBS: Na_2HPO_4/NaH_2PO_4, 1.0 M, pH 4.12) was used as the electrolyte for GO electrochemical reduction. Doubly distilled water was used throughout the work. GO was prepared from natural graphite powder by a modified Hummers method, as described in the Supporting Information.[30,31] To obtain a GO aqueous dispersion, 12 mg of as-prepared GO was dispersed in 40 mL of doubly distilled water under ultrasonication for 2 h to form a 0.3 mg mL^{-1} GO suspension.

2.2. Preparation of PtPd/RGO. The whole preparation processes for constructing the PtPd/RGO catalyst is illustrated in Scheme 1. First, an aqueous solution of 0.65 mL of H_2PtCl_6 (7.723×10^{-3} mol L^{-1}) and 0.22 mL of H_2PdCl_4 (22.55×10^{-3} mol L^{-1}) with a Pt-to-Pd molar ratio of 1:1 was added into the GO solution with stirring for 30 min so that they were mixed thoroughly. Subsequently, H_2 was bubbled through the solution under constant stirring for 4 h to ensure the complete reduction of metal precursors. UV−vis absorption spectra were employed to detect whether these metal precursors were reduced completely. The obtained sample from this reduction step is denoted PtPd (1:1)/GO. Finally, GO was reduced by dropping 20 μL

of the PtPd (1:1)/GO suspension onto the glassy carbon electrode (GC) and drying at room temperature, which was then reduced at a constant potential of −0.9 V for 1000 s in Na-PBS solution (denoted PtPd (1:1)/RGO). The reduction of GO was confirmed by Raman spectroscopy, and the results are shown in Figure S1 (Supporting Information). For comparison, Pt/RGO, Pd/RGO, PtPd (3:1)/RGO, and PtPd (1:3)/RGO catalysts were also prepared in the same way. All of the catalysts have a metal (Pt + Pd) loading of 11 wt %.

2.3. Instrumentation and Characterization. All electrochemical measurements were carried out on a CHI 660B electrochemical workstation (Shanghai Chenhua Instrumental Co., Ltd, China) at room temperature. A conventional three-electrode system was used, with a glassy carbon electrode (GC, 3 mm diameter) as the working electrode, platinum wire as the counter electrode, and a saturated calomel electrode (SCE) as the reference. All solutions were deaerated by a dry nitrogen stream and maintained with a slight overpressure of nitrogen during the entire experiment. UV−vis absorption spectra of the samples were recorded on a TU1810 SPC spectrometer. Transmission electron microscopy (TEM) measurements were carried out with a TECNAI-G20 electron microscope with an accelerating voltage of 200 kV. High-resolution TEM (HRTEM) images were obtained with a JEM-2100F high-resolution transmission electron microscope operating at 200 kV. X-ray diffraction (XRD) patterns of the catalysts were measured on a PANalytical X'Pert PRO MRD X-ray diffractometer using Cu Kα as the radiation source (λ = 1.54056 Å). The Raman spectra were recorded on a Renishaw inVia plus Raman microscope using a 633 nm argon ion laser. X-ray photoelectron spectroscopy (XPS) measurements were performed on an ESCALab220i-XL electron spectrometer from VG Scientific using 300 W Al Kα X-ray radiation as the X-ray source for excitation. The actual loading and composition of Pt and Pd in the as-prepared PtPd/RGO catalysts were determined by inductively coupled plasma atomic emission spectrometry (ICP−AES), and the data are summarized in Table 1.

Table 1. Summary of the Loading and Composition Data for the Catalysts on the Basis of ICP Analysis

		metal loading (μg cm^{-2})	
catalysts	molar ratio (Pt/Pd)	Pt	Pd
Pt/RGO		10.52	
Pd/RGO			10.62
Pt−Pd (3:1)/RGO	3.00:0.98	8.93	1.60
Pt−Pd (1:1)/RGO	1.00:1.00	6.85	3.71
Pt−Pd (1:3)/RGO	1.00:3.10	3.99	6.59

3. RESULTS AND DISCUSSION

Figure 1 shows the digital photos of GO (a), Pt/GO (b), Pd/GO (c), Pt−Pd (3:1)/GO (d), Pt−Pd (1:1)/GO (e), and Pt−Pd (1:3)/GO (f). It can be seen from Figure 1 sample a that the as-prepared GO can be well-dispersed in water with the aid of sonication to form a stable light brown suspension that is maintained for several months. After H_2 is bubbled through the mixture solutions of GO + H_2PtCl_6 or/and H_2PdCl_4 under constant stirring for 4 h, the color of the solutions changed from light brown to black, indicating the successful formation of Pt or/and Pd NPs. The as-prepared Pt/GO, Pd/GO, Pt−Pd (3:1)/GO, Pt−Pd (1:1)/GO, and Pt−Pd (1:3)/GO can also form stable suspensions that are maintained for several months, as shown in Figure 1, samples b−f, respectively, without any stabilizers.

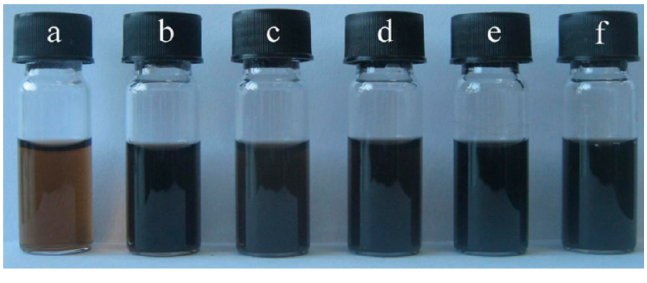

Figure 1. Digital photos of GO (a), Pt/GO (b), Pd/GO (c), Pt−Pd (3:1)/GO (d), Pt−Pd (1:1)/GO (e), and Pt−Pd (1:3)/GO (f).

UV−vis absorption spectra were employed to detect whether the precursors, H_2PtCl_6 and H_2PdCl_4, are reduced to Pt and Pd NPs. Figure 2 depicts the UV−vis absorption spectra of the H_2PtCl_6 and H_2PdCl_4 precursors as well as those of GO, Pt/GO, Pd/GO, Pt−Pd (1:1)/GO, Pt−Pd (3:1)/GO, and Pt−Pd (1:3)/GO. As shown in Figure 2A, an absorption peak located at around 260 nm can be observed for the H_2PtCl_6 solution, which is attributed to the absorption of Pt^{4+} ions.[32] For H_2PdCl_4, the distinct absorption peak appears at around 210 nm.[33] In addition, GO shows a prominent absorption peak at 230 nm.[34] After H_2 reduction, the peak at 260 nm disappears for Pt/GO, and only the peak at 230 nm is observed (absorption peak of GO), indicating that the reduction of Pt^{4+} to Pt and the existence of GO. Similar phenomena occurred for Pd/GO, Pt−Pd (1:1)/GO, Pt−Pd (3:1)/GO, and Pt−Pd (1:3)/GO. Accordingly, these results confirm that Pt and Pd precursors have been successfully reduced.

The morphology and structural features of the Pt/GO, Pd/GO, Pt−Pd (1:1)/GO, Pt−Pd (1:3)/GO, and Pt−Pd (3:1)/GO catalysts were elucidated by transmission electron microscopy (TEM) analysis. Typical TEM images are shown in Figure 3. It can be observed from the TEM images in Figure 3a−e that the metallic NPs are nearly spherical in shape and homogeneously dispersed on the GO support without obvious agglomeration. This is probably due to the surface functional groups, such as carbonyl (−C═O) and carboxylic (−COOH) groups, which may help the metal NPs to absorb to the surface of the GO. The average sizes of the metallic NPs in the Pt/GO, Pd/GO, Pt−Pd (1:1)/GO, Pt−Pd (1:3)/GO, and Pt−Pd (3:1)/GO catalysts estimated from their histograms (Figure S2, Supporting Information) are approximately 7.03, 5.16, 4.54, 3.99, and 4.79 nm, respectively, of which Pt−Pd (1:3)/GO displays the smallest particle size, suggesting that it may has more active sites and could help to enhance catalytic activity. High-resolution TEM (HRTEM) images in Figure 3a′−e′ further reveal that the metallic NPs are crystalline with clear lattice structures. The HRTEM image in Figure 1a′ reveals a clear lattice distance of ∼0.229 nm, corresponding to the (111) lattice plane of the face-centered cubic (fcc) structure of Pt.[35] Figure 3b′ shows the HRTEM image of Pd NPs with a lattice distance of ∼0.220 nm, which matches well with the (111) plane of fcc Pd.[36] The lattice spacing for Pt−Pd (1:1), Pt−Pd (1:3), and Pt−Pd (3:1) are 0.225, 0.228, and 0.222 nm, respectively, which are between that of monometallic Pt and Pd, indicating the formation of PtPd alloy.

The crystal structures of the as-prepared Pt/GO, Pd/GO, Pt−Pd (1:1)/GO, Pt−Pd (1:3)/GO, and Pt−Pd (3:1)/GO catalysts were further characterized by X-ray diffraction (XRD), and the XRD patterns are shown in Figure 4. As shown in Figure 4A, all of the catalysts display a typical fcc structure. For the monometallic Pt, the diffraction peaks located at the 2θ values of 39.94, 46.69, and 67.17° are assigned to Pt (111), (200), and (220) lattice planes, respectively (JCPDS 04-

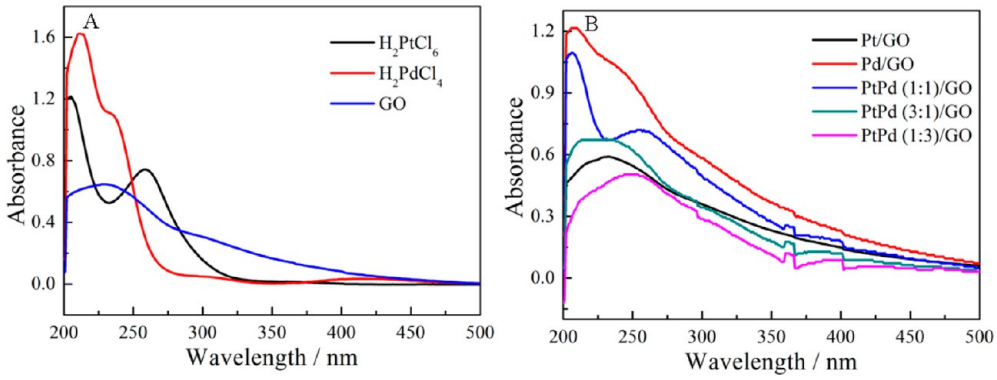

Figure 2. UV−vis spectra of (A) H_2PtCl_6, H_2PdCl_4, and GO and (B) Pt, Pd, Pt−Pd (1:1), Pt−Pd (3:1), and Pt−Pd (1:3).

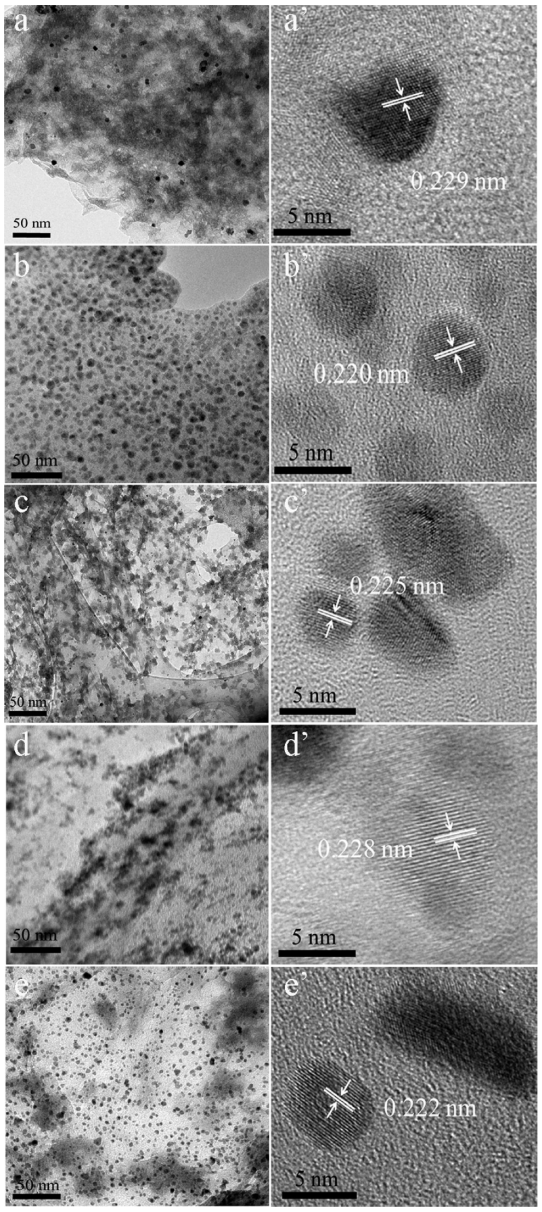

Figure 3. TEM images of Pt/GO (a), Pd/GO (b), Pt−Pd (1:1)/GO (c), Pt−Pd (1:3)/GO (d), and Pt−Pd (3:1)/GO (e). HRTEM images of Pt/GO (a′), Pd/GO (b′), Pt−Pd (1:1)/GO (c′), Pt−Pd (1:3)/GO (d′), and Pt−Pd (3:1)/GO (e′).

0802).[37] In the case of monometallic Pd, the peaks at about 40.32, 46.92, and 67.98° are attributed to the (111), (200) and (220) lattice planes of the fcc crystalline structure of Pd, respectively (JCPDS 46-1043).[38] For the binary systems, the XRD patterns of the PtPd/GO with three different Pt/Pd ratios (1:1, 1:3, and 3:1) are similar to those of the pure Pt or Pd catalyst. For clear observation, the magnified (111) peaks of these catalysts are enlarged in Figure 4B. The 2θ values of the (111) peak for the binary systems, Pt−Pd (1:1), Pt−Pd (1:3), and Pt−Pd (3:1) catalysts, were observed to be 40.08, 40.21, and 40.04°, respectively, indicating peak positioning in between the pure metallic phases. Similar results have been also observed in other bimetallic alloy nanostructures. Additionally, with the increase in the Pd ratio, the peak positions slightly shift higher. Overall, these results demonstrate the successful formation of PtPd alloys.

X-ray photoelectron spectroscopy (XPS) measurements were also used to elucidate the composition and surface oxidation states of the as-prepared catalysts. Figure 5A shows the Pt 4f XPS spectra of Pt/GO, Pt−Pd (3:1)/GO, Pt−Pd (1:1)/GO, and Pt−Pd (1:3)/GO. From Figure 5A, it can be clearly seen that the XPS spectrum of Pt/GO displays two prominent peaks located at binding energies of 71.3 and 74.5 eV, corresponding to the Pt $4f_{7/2}$ and Pt $4f_{5/2}$ of metallic Pt, whereas the other two weaker peaks at 70.0 and 73.6 eV can be assigned to Pt oxide, such as PtO_2 and PtO.[39,40] Compared with the XPS spectrum of monometallic Pt, the Pt 4f peak slightly shifts toward lower values for the binary PtPd catalysts (Pt−Pd (3:1)/GO, Pt−Pd (1:1)/GO, and Pt−Pd (1:3)/GO). Additionally, the shift of the peak increased with an increase in the Pd content. The Pd 3d spectra of Pd/GO, Pt−Pd (3:1)/GO, Pt−Pd (1:1)/GO, and Pt−Pd (1:3)/GO are given in Figure 5B. For the Pd/GO catalyst, the two peaks at 335.45 and 340.65 eV seen in Figure 5B correspond to Pd $3d_{5/2}$ and Pd $3d_{3/2}$, respectively, which indicates that Pd exists only in a metallic state without any surface oxide.[41] All of the catalysts have similar Pd 3d profiles. Meanwhile, it can be clearly seen that the binding energies of Pd 3d for the binary PtPd catalysts with different Pt/Pd ratios (1:1, 1:3, and 3:1) also gradually shift to a lower binding energy relative to that of pure Pd as the Pt content increases. Together, the shifts in the binding energy for Pt and Pd in binary PtPd catalysts indicate a change in the electronic structure of Pt and Pd, which could be ascribed to the electronic interactions between Pt and Pd atomic orbitals, leading to electron transfer from Pd to Pt (electronegativity: Pt, 2.28; Pd, 2.20).[42] The increased electron density around Pt would then cause partial filling of Pt 5d bands, resulting in the downward shift of the d-

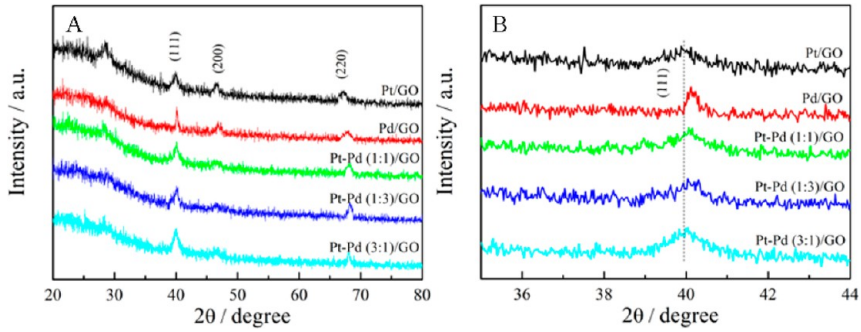

Figure 4. (A) XRD patterns of Pt/GO, Pd/GO, Pt−Pd (1:1)/GO, Pt−Pd (1:3)/GO, and Pt−Pd (3:1)/GO catalysts and (B) enlarged patterns of the (111) peaks.

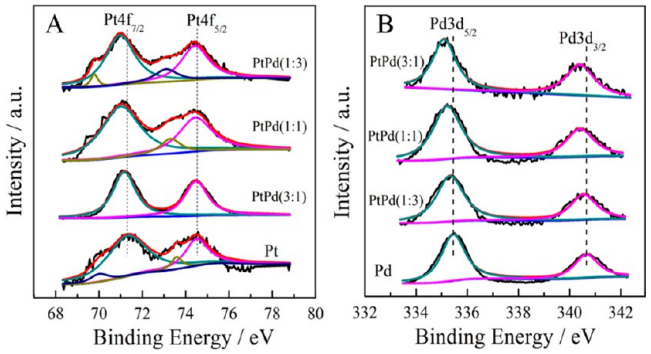

Figure 5. (A) Pt 4f XPS spectra of Pt/GO, Pt−Pd (3:1)/GO, Pt−Pd (1:1)/GO, and Pt−Pd (1:3)/GO and (B) Pd 3d XPS spectra of Pd/GO, Pt−Pd (3:1)/GO, Pt−Pd (1:1)/GO, and Pt−Pd (1:3)/GO.

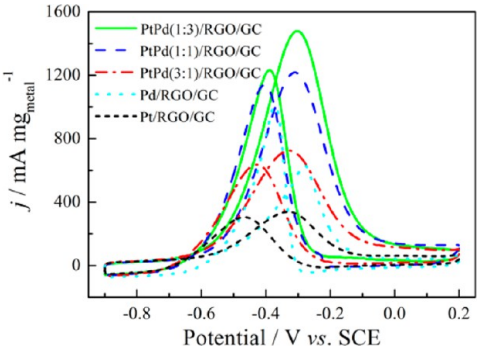

Figure 6. CV curves of Pt−Pd (1:3)/RGO/GC, Pt−Pd (1:1)/RGO/GC, Pt−Pd (3:1)/RGO/GC, Pd/RGO/GC, and Pt/RGO/GC catalysts in 1.0 M EtOH + 1.0 M KOH at a scan rate of 50 mV s^{-1} (metal: total metal loading of Pt and Pd).

band center and the weakening of CO adsorption on Pt and potentially decreasing the CO poisoning effect, thus enhancing the activity and durability toward ethanol oxidation.[43] The XPS results also strongly suggest the formation of PtPd alloys, as such a variation in binding energy has been observed for the bimetallic PtAu and PtRu particles in other reports.[44,45]

Prior to the electrocatalytic oxidation of ethanol, CV curves of the Pt−Pd (1:3)/RGO/GC, Pt−Pd (1:1)/RGO/GC, Pt−Pd (3:1)/RGO/GC, Pd/RGO/GC, and Pt/RGO/GC catalysts were obtained in 1.0 M KOH at a scan rate of 50 mV s^{-1} and are displayed in Figure S3 (Supporting Information). Generally, the electrochemical active surface area (ECSA) of the catalyst is a key parameter for electrocatalytic activity and can be calculated by integrating the charge (Q_H) on hydrogen adsorption−desorption regions by cyclic voltammetry. Pt−Pd (1:3)/RGO/GC presents the largest ECSA value, which could be attributed to the smaller size and better distribution of the PtPd NPs.

The electrocatalytic activities of the Pt−Pd (1:3)/RGO/GC, Pt−Pd (1:1)/RGO/GC, Pt−Pd (3:1)/RGO/GC, Pd/RGO/GC, and Pt/RGO/GC catalysts were evaluated by cyclic voltammetry in a 1.0 M KOH + 1.0 M ethanol solution at a scan rate of 50 mV s^{-1}. The current density was normalized on the basis of the total mass of the metals so that the current density (j) can be directly used to compare the catalytic activity of different catalysts. The current density normalized to the ECSA is displayed in Figure S4 (Supporting Information). As shown in Figure 6, two well-defined oxidation peaks can be clearly observed: one in the forward scan is produced because of the oxidation of freshly chemisorbed species coming from ethanol adsorption, whereas the other in the reverse scan is primarily ascribed to the removal of the incompletely oxidized carbonaceous species formed during the forward scan.[46] Thus, the oxidation peak during the forward scan is usually used to evaluate the catalytic activity of the catalyst. It was observed that the Pd/RGO/GC catalyst shows higher catalytic activity toward ethanol oxidation than Pt/RGO/GC, which is in agreement with other reported results.[47] Moreover, the PtPd binary catalysts (Pt−Pd (1:3)/RGO/GC, Pt−Pd (1:1)/RGO/GC, and Pt−Pd (3:1)/RGO/GC) exhibit considerable improvements over that of pure Pt and Pd (Pt/RGO/GC and Pd/RGO/GC). In particular, the forward peak current density of the Pt−Pd (1:3)/RGO/GC catalyst reaches a value of 1486.7 mA mg_{metal}^{-1}, which is about 1.20-, 2.03-, 2.30-, and 4.30-fold as large as those of Pt−Pd (1:1)/RGO/GC (1224.4 mA mg_{metal}^{-1}), Pt−Pd (3:1)/RGO/GC (732.9 mA mg_{metal}^{-1}), Pd/RGO/GC (645.5 mA mg_{metal}^{-1}), and Pt/RGO/GC (345.7 mA mg_{metal}^{-1}), respectively. The enhanced catalytic activity of bimetallic over pure metals could be ascribed to two possible explanations: (1) the synergistic effect between Pt and Pd, which has also been affirmed by other groups[48,49] and to (2) the ligand effect. According to the d-band theory of Hammer−Nørskov,[50,51] the d-band center of Pd will be shifted upward when it is combined with Pt because the lattice constant of Pt (3.92 Å) is larger than that of Pd (3.89 Å), which is consistent with the XPS observation of the negative shift of the binding energy for Pd in binary PtPd catalysts. This could promote the adsorption of OH^-, which would facilitate the oxidation of CH_3CO_{ads} and thus help to enhance the ethanol oxidation process. However, excess adsorption of OH^- also causes a competition with the adsorption of ethanol.[52] This could be a possible reason for the activity decrease on the catalysts when the Pt content continued to increase. Additionally, the current

dx.doi.org/10.1021/am405846h | ACS Appl. Mater. Interfaces 2014, 6, 3607−3614

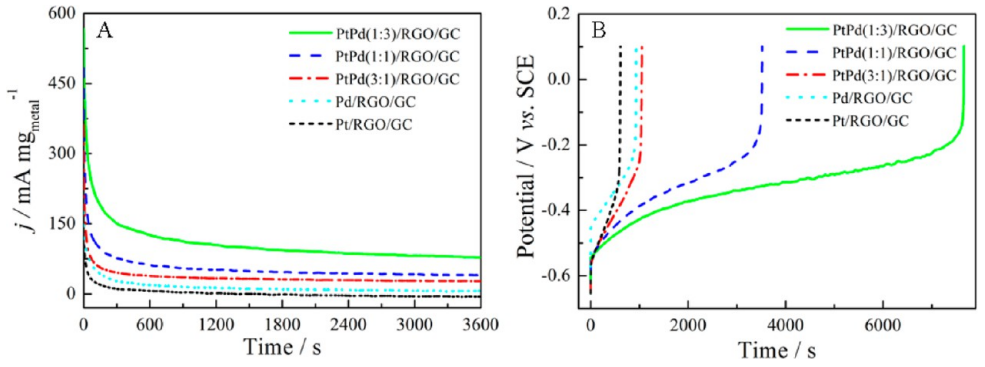

Figure 7. (A) Chronoamperometric curves of ethanol oxidation at Pt−Pd (1:3)/RGO/GC, Pt−Pd (1:1)/RGO/GC, Pt−Pd (3:1)/RGO/GC, Pd/RGO/GC, and Pt/RGO/GC in 1.0 M EtOH + 1.0 M KOH at −0.35 V and (B) chronopotentiometric curves of ethanol oxidation on Pt−Pd (1:3)/RGO/GC, Pt−Pd (1:1)/RGO/GC, Pt−Pd (3:1)/RGO/GC, Pd/RGO/GC, and Pt/RGO/GC in 1.0 M EtOH + 1.0 M KOH at 0.4 mA cm^{-2} (metal: total metal loading of Pt and Pd).

density of Pt−Pd (1:3)/RGO/GC is also higher than that of commercial JM 20 wt % Pt/C/GC and JM 20 wt % Pd/C/GC (see Figure S5 in the Supporting Information) as well as of many previously reported PtPd composites such as Pt/Pd bimetallic nanotubes (1160 mA mg_{metal}^{-1}),[53] PdPt alloy nanowires (950 mA mg_{metal}^{-1}),[54] and other PtPd catalysts,[13,49,55,56] indicating that the as prepared Pt−Pd (1:3)/RGO/GC catalyst possesses an excellent catalytic activity.

The antipoisoning abilities of the Pt−Pd (1:3)/RGO/GC, Pt−Pd (1:1)/RGO/GC, Pt−Pd (3:1)/RGO/GC, Pd/RGO/GC, and Pt/RGO/GC electrodes for ethanol oxidation were evaluated by chronoamperometric measurements at a potential of −0.35 V for 3600 s in 1.0 M EtOH + 1.0 M KOH, and the results are shown in Figure 7A. An initially rapid current decay for all catalysts was observed, probably because of the accumulations of poisonous carbonaceous intermediates (such as CO_{ads}, CH_3CHO_{ads}, etc.) on the catalyst surface during the ethanol oxidation reaction, similar to what has been reported.[42] Obviously, during the whole time, the current density of ethanol oxidation on Pt−Pd (1:3)/RGO/GC is higher and the current density decay is significantly slower than those on the Pt−Pd (1:1)/RGO/GC, Pt−Pd (3:1)/RGO/GC, Pd/RGO/GC, and Pt/RGO/GC catalysts, demonstrating that the Pt−Pd (1:3)/RGO/GC catalyst has a relatively higher catalytic activity and better stability for ethanol oxidation as compared to the other catalysts, which is consistent with the CV results displayed in Figure 6. Chronopotentiometry was then performed to examine the durability of catalysts further. Figure 7B presents the chronopotentiometric curves of Pt−Pd (1:3)/RGO/GC, Pt−Pd (1:1)/RGO/GC, Pt−Pd (3:1)/RGO/GC, Pd/RGO/GC, and Pt/RGO/GC at 0.4 mA cm^{-2} in 1.0 M EtOH + 1.0 M KOH. The potential increases with the polarization time and finally shifts to a higher potential for oxygen evolution, indicating the poisoning of the catalysts.[57] The time at which the electrode potential jumps to a higher potential can be used to evaluate the antipoisoning ability of a catalyst.[58] For the Pt−Pd (1:3)/RGO/GC electrode, the sustained time is 7663 s, which is longer than that for Pt−Pd (1:1)/RGO/GC (3518 s), Pt−Pd (3:1)/RGO/GC (1052 s), Pd/RGO/GC (933 s), and Pt/RGO/GC (611 s), further indicating that Pt−Pd (1:3)/RGO/GC has a better poisoning-tolerance capability for ethanol oxidation.

For practical applications, the long-term stability of the electrode is of great importance. With this in mind, CV scans of 100 cycles were performed on the Pt−Pd (1:3)/RGO, Pt−Pd (1:1)/RGO/GC, Pt−Pd (3:1)/RGO/GC, Pd/RGO/GC, and Pt/RGO/GC electrodes in a 1.0 M EtOH + 1.0 M KOH solution at 50 mV s^{-1}. Figure 8 shows the forward peak current

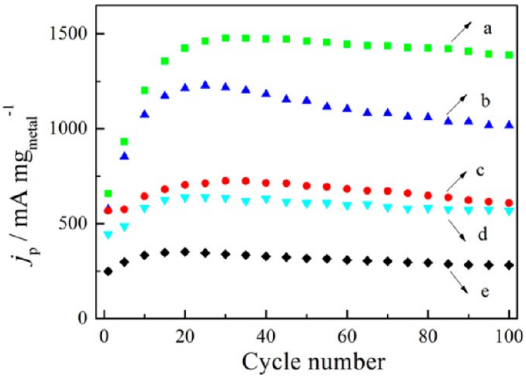

Figure 8. Peak current of ethanol oxidation in the forward scan on Pt−Pd (1:3)/RGO/GC (a), Pt−Pd (1:1)/RGO/GC (b), Pt−Pd (3:1)/RGO/GC (c), Pd/RGO/GC (d), and Pt/RGO/GC (e) vs the CV cycle number in a 1.0 M EtOH + 1.0 M KOH solution (metal: total metal loading of Pt and Pd).

density as a function of cycle scan number. For all catalysts, it can be observed that the forward oxidation peak current density increases with the increase of the scan number at the initial stage and then decreases gradually as the number of scans further increase. In the case of Pt−Pd (1:3)/RGO/GC, the forward peak current density reaches the maximum (1478.1 mA mg_{metal}^{-1}) at the 30th cycle and then decreases slowly as the number of scans continues. After 100 cycles, the Pt−Pd (1:3)/RGO/GC still demonstrates a high peak current density (1389.4 mA mg_{metal}^{-1}) as compared to Pt−Pd (1:1)/RGO/GC (1017.2 mA mg_{metal}^{-1}), Pt−Pd (3:1)/RGO/GC (609.2 mA mg_{metal}^{-1}), Pd/RGO/GC (568.0 mA mg_{metal}^{-1}), and Pt/RGO/GC (280.8 mA mg_{metal}^{-1}), which has a total decrease of 6% relative to its maximum value. However, the values for the Pt−Pd (1:1)/RGO/GC, Pt−Pd (3:1)/RGO/GC, Pd/RGO/GC, and Pt/RGO/GC electrodes are 17.2, 16.1, 11.4, and 21%, respectively. These observations clearly reveal that Pt−Pd (1:3)/RGO/GC has a much higher catalytic activity and better stability for ethanol oxidation in alkaline medium than those of the other four electrodes.

4. CONCLUSIONS

We have developed a facile and environmentally friendly method for synthesizing PtPd alloy catalysts with different Pt/Pd ratios in the absence of any stabilizers or surfactants that ensures that the as-prepared catalysts have a clean surface and allows them to demonstrate a high electrocatalytic activity for ethanol oxidation. XRD results suggest that the PtPd NPs formed an alloy structure. TEM and HRTEM show that the synthesized PtPd NPs deposited on the surface of GO are smaller in size, ~4−7 nm, and exhibit clear lattice spacings. The present study is important because it can be readily extended to the synthesis of other alloy NPs on RGO for electro-oxidation, electrochemical sensors, and other catalysis-related areas. Work to explore these bimetallic PtPd NPs for various chemical reactions is underway.

■ ASSOCIATED CONTENT

Supporting Information

Preparation of GO; Raman spectra of GO and as-prepared catalysts; size distributions of the Pt/GO, Pd/GO, Pt−Pd (1:1)/GO, Pt−Pd (1:3)/GO, and Pt−Pd (3:1)/GO nanoparticles; CV curves of as-prepared catalysts in 1.0 M KOH; CV curves of as-prepared catalysts in 1.0 M EtOH + 1.0 M KOH; and CV curves of JM 20 wt % Pt/C/GC and JM 20 wt % Pd/C/GC for ethanol oxidation. This material is available free of charge via the Internet at http://pubs.acs.org.

■ AUTHOR INFORMATION

Corresponding Authors

*E-mail: duyk@suda.edu.cn (Y.D.).
*E-mail: xujingkun@tsinghua.org.cn (J.X.).
*E-mail: luwensheng@iccas.ac.cn (W.L.).

Notes

The authors declare no competing financial interest.

■ ACKNOWLEDGMENTS

This work was supported by the National Natural Science Foundation of China (grant nos. 51073114, 20933007, and 51373111), the Opening Project of Xinjiang Key Laboratory of Electronic Information Materials and Devices (XJYS0901-2010-01), the Priority Academic Program Development of Jiangsu Higher Education Institutions (PAPD), and the Academic Award for Young Graduate Scholar of Soochow University.

■ REFERENCES

(1) Hosseini, M. G.; Momeni, M. M. UV-Cleaning Properties of Pt Nanoparticle-Decorated Titania Nanotubes in the Electro-Oxidation of Methanol: An Anti-Poisoning and Refreshable Electrode. *Electrochim. Acta* **2012**, *70*, 1−9.

(2) Zhang, S.; Shao, Y. Y.; Liao, H.G.; Liu, J.; Aksay, I. A.; Yin, G. P.; Lin, Y. H. Graphene Decorated with PtAu Alloy Nanoparticles: Facile Synthesis and Promising Application for Formic Acid Oxidation. *Chem. Mater.* **2011**, *23*, 1079−1081.

(3) Singh, R. N.; Singh, A.; Anindita. Electrocatalytic Activity of Binary and Ternary Composite Films of Pd, MWCNT, and Ni for Ethanol Electro-Oxidation in Alkaline Solutions. *Carbon* **2009**, *47*, 271−278.

(4) Zhou, W. J.; Zhou, Z. H.; Song, S. Q.; Li, W. Z.; Sun, G. Q.; Tsiakaras, P.; Xin, Q. Pt Based Anode Catalysts for Direct Ethanol Fuel Cells. *Appl. Catal., B* **2003**, *46*, 273−285.

(5) Song, H. Q.; Qiu, X. P.; Li, F. S. Promotion of Carbon Nanotube-Supported Pt Catalyst for Methanol and Ethanol Electro-Oxidation by ZrO_2 in Acidic Media. *Appl. Catal., A* **2009**, *364*, 1−7.

(6) Xue, X. Z.; Ge, J. J.; Tian, T.; Liu, C. P.; Xing, W.; Lu, T. H. Enhancement of the Electrooxidation of Ethanol on Pt-Sn-P/C Catalysts Prepared by Chemical Deposition Process. *J. Power Sources* **2007**, *172*, 560−569.

(7) Jiang, L.; Hsu, A.; Chu, D.; Chen, R. Ethanol Electro-Oxidation on Pt/C and PtSn/C Catalysts in Alkaline and Acid Solutions. *Int. J. Hydrogen Energy* **2010**, *35*, 365−372.

(8) Spendelow, J. S.; Wieckowski, A. Electrocatalysis of Oxygen Reduction and Small Alcohol Oxidation in Alkaline Media. *Phys. Chem. Chem. Phys.* **2007**, *9*, 2654−2675.

(9) Huang, Y. Y.; Cai, J. D.; Guo, Y. L. A High-Efficiency Microwave Approach to Synthesis of Bi-Modified Pt Nanoparticle Catalysts for Ethanol Electro-Oxidation in Alkaline Medium. *Appl. Catal., B* **2013**, *129*, 549−555.

(10) Silva, J. C. M.; Parreira, L. S.; De Souza, R. F. B.; Calegaro, M. L.; Spinacé, E. V.; Neto, A. O.; Santos, M. C. PtSn/C Alloyed and Non-Alloyed Materials: Differences in the Ethanol Electro-Oxidation Reaction Pathways. *Appl. Catal., B* **2011**, *110*, 141−147.

(11) Zhao, Y. C.; Yang, X. L.; Zhan, L.; Ou, S. J.; Tian, J. N. High Electrocatalytic Activity of PtRu Nanoparticles Supported on Starch-Functionalized Multi-Walled Carbon Nanotubes for Ethanol Oxidation. *J. Mater. Chem.* **2011**, *21*, 4257−4261.

(12) Habibi, B.; Dadashpour, E. Carbon-Cceramic Supported Bimetallic Pt-Ni Nanoparticles as an Electrocatalyst for Electrooxidation of Methanol and Ethanol in Acidic Media. *Int. J. Hydrogen Energy* **2013**, *38*, 5425−5434.

(13) Lin, S. C.; Chen, J. Y.; Hsieh, Y. F.; Wu, P. W. A Facile Route to Prepare PdPt Alloys for Ethanol Electro-Oxidation in Alkaline Electrolyte. *Mater. Lett.* **2011**, *65*, 215−218.

(14) Liang, Z. X.; Zhao, T. S.; Xu, J.B.; Zhu, L. D. Mechanism Study of the Ethanol Oxidation Reaction on Palladium in Alkaline Media. *Electrochim. Acta* **2009**, *54*, 2203−2208.

(15) Fang, X.; Wang, L.; Shen, P. K.; Cui, G.; Bianchini, C. An In Situ Fourier Transform Infrared Spectroelectrochemical Study on Ethanol Electrooxidation on Pd in Alkaline Solution. *J. Power Sources* **2010**, *195*, 1375−1378.

(16) Antolini, E. Palladium in Fuel Cell Catalysis. *Energy Environ. Sci.* **2009**, *2*, 915−931.

(17) Hu, Y. J.; Zhang, H.; Wu, P.; Zhang, H.; Zhou, B.; Cai, C. X. Bimetallic Pt-Au Nanocatalysts Electrochemically Deposited on Graphene and Their Electrocatalytic Characteristics towards Oxygen Reduction and Methanol Oxidation. *Phys. Chem. Chem. Phys.* **2011**, *13*, 4083−4094.

(18) Ren, F. F.; Wang, C. Q.; Zhai, C. Y.; Jiang, F. X.; Yue, R. R.; Du, Y. K.; Yang, P.; Xu, J. K. One-Pot Synthesis of a RGO-Supported Ultrafine Ternary PtAuRu Catalyst with High Electrocatalytic Activity towards Methanol Oxidation in Alkaline Medium. *J. Mater. Chem. A* **2013**, *1*, 7255−7261.

(19) Bai, Z. Y.; Yang, L.; Guo, Y. M.; Zheng, Z.; Hu, C. G.; Xu, P. L. High-Efficiency Palladium Catalysts Supported on PPY-Modified C_{60} for Formic Acid Oxidation. *Chem. Commun.* **2011**, *47*, 1752−1754.

(20) Wu, B. H.; Hu, D.; Kuang, Y. J.; Yu, Y. M.; Zhang, X. H.; Chen, J. H. High Dispersion of Platinum-Ruthenium Nanoparticles on the 3,4,9,10-Perylene Tetracarboxylic Acid-Functionalized Carbon Nanotubes for Methanol Electro-Oxidation. *Chem. Commun.* **2011**, *47*, 5253−5255.

(21) Tsai, M. C.; Yeh, T. K.; Tsai, C. H. An Improved Electrodeposition Technique for Preparing Platinum and Platinum-Ruthenium Nanoparticles on Carbon Nanotubes Directly Grown on Carbon Cloth for Methanol Oxidation. *Electrochem. Commun.* **2006**, *8*, 1445−1452.

(22) Guo, S. J.; Dong, S. J.; Wang, E. Three-Dimensional Pt-on-Pd Bimetallic Nanodendrites Supported on Graphene Nanosheet: Facile Synthesis and Used as an Advanced Nanoelectrocatalyst for Methanol Oxidation. *ACS Nano* **2010**, *4*, 547−555.

(23) Muszynski, R.; Seger, B.; Kamat, P. V. Decorating Graphene Sheets with Gold Nanoparticles. *J. Phys. Chem. C* **2008**, *112*, 5263−5266.

(24) Hsieh, C.T.; Chen, W. Y.; Tzou, D. Y.; Roy, A. K.; Hsiao, H. T. Atomic Layer Deposition of Pt Nanocatalysts on Graphene Oxide Nanosheets for Electro-Oxidation of Formic Acid. *Int. J. Hydrogen Energy* **2012**, *37*, 17837−17843.
(25) Wen, Z. L.; Yang, S. D.; Liang, Y. Y.; He, W.; Tong, H.; Hao, L.; Zhang, X. G.; Song, Q. J. The Improved Electrocatalytic Activity of Palladium/Graphene Nanosheets towards Ethanol Oxidation by Tin Oxide. *Electrochim. Acta* **2010**, *56*, 139−144.
(26) Fu, B. S.; Missaghi, M. N.; Downing, C. M.; Kung, M. C.; Kung, H. H.; Xiao, G. M. Engineered Polymer for Controlled Metal Nanoparticle Synthesis. *Chem. Mater.* **2010**, *22*, 2181−2183.
(27) Carpenter, M. K.; Moylan, T. E.; Kukreja, R. S.; Atwan, M. H.; Tessema, M. M. Solvothermal Synthesis of Platinum Alloy Nanoparticles for Oxygen Reduction Electrocatalysis. *J. Am. Chem. Soc.* **2012**, *134*, 8535−8542.
(28) Wu, J.; Zhang, J.; Peng, Z.; Yang, S.; Wagner, F. T.; Yang, H. Truncated Octahedral Pt_3Ni Oxygen Reduction Reaction Electrocatalysts. *J. Am. Chem. Soc.* **2010**, *132*, 4984−4985.
(29) Merga, G.; Saucedo, N.; Cass, L. C.; Puthussery, J.; Meisel, D. "Naked" Gold Nanoparticles: Synthesis, Characterization, Catalytic Hydrogen Evolution, and SERS. *J. Phys. Chem. C* **2010**, *114*, 14811−14818.
(30) Yao, Z. Q.; Zhu, M. S.; Jiang, F. X.; Du, Y. K.; Wang, C. Y.; Yang, P. Highly Efficient Electrocatalytic Performance Based on Pt Nanoflowers Modified Reduced Graphene Oxide/Carbon Cloth Electrode. *J. Mater. Chem.* **2012**, *22*, 13707−13713.
(31) Li, D.; Muller, M. B.; Gilje, S.; Kaner, R. B.; Wallace, G. G. Processable Aqueous Dispersions of Graphene Nanosheets. *Nat. Nanotechnol.* **2008**, *3*, 101−105.
(32) Li, L. R.; Huang, M. H.; Liu, J. J.; Guo, Y. L. Pt_xSn/C Electrocatalysts Synthesized by Improved Microemulsion Method and Their Catalytic Activity for Ethanol Oxidation. *J. Power Sources* **2011**, *196*, 1090−1096.
(33) Ding, K. Q.; Wang, Y. H.; Yang, H. W.; Zheng, C. B.; Cao, Y. L.; Wei, H. G.; Wang, Y. R.; Guo, Z. H. Electrocatalytic Activity of Multi-Walled Carbon Nanotubes-Supported Pt_xPd_y Catalysts Prepared by a Pyrolysis Process toward Ethanol Oxidation Reaction. *Electrochim. Acta* **2013**, *100*, 147−156.
(34) Zhao, X. M.; Zhou, S. W.; Shen, Q. M.; Jiang, L. P.; Zhu, J. J. Fabrication of Glutathione Photoelectrochemical Biosensor Using Graphene-CdS Nanocomposites. *Analyst* **2012**, *137*, 3697−3703.
(35) Qiu, H. J.; Dong, X. C.; Sana, B.; Peng, T.; Paramelle, D.; Chen, P.; Lim, S. Ferritin-Templated Synthesis and Self-Assembly of Pt Nanoparticles on a Monolithic Porous Graphene Network for Electrocatalysis in Fuel Cells. *ACS Appl. Mater. Interfaces* **2013**, *5*, 782−787.
(36) Chen, X. M.; Wu, G. H.; Chen, J. M.; Chen, X.; Xie, Z. X.; Wang, X. R. Synthesis of "Clean" and Well-Dispersive Pd Nanoparticles with Excellent Electrocatalytic Property on Graphene Oxide. *J. Am. Chem. Soc.* **2011**, *133*, 3693−3695.
(37) Luo, B. M.; Xu, S.; Yan, X. B.; Xue, Q. J. Synthesis and Electrochemical Properties of Graphene Supported PtNi Nanodendrites. *Electrochem. Commun.* **2012**, *23*, 72−75.
(38) Huang, H. J.; Wang, X. Pd Nanoparticles Supported on Low-Defect Graphene Sheets: For Use as High-Performance Electrocatalysts for Formic Acid and Methanol Oxidation. *J. Mater. Chem.* **2012**, *22*, 22533−22541.
(39) Jeon, M. K.; Kang, M. Effect of Pt Addition on Vanadium-Incorporated TiO_2 Catalysts for Photodecomposition of Ammonia. *Korean J. Chem. Eng.* **2007**, *24*, 774−780.
(40) Fıçıcılar, B.; Bayrakçeken, A.; Eroğlu, İ. Effect of Pd Loading in Pd-Pt Bimetallic Catalysts Doped into Hollow Core Mesoporous Shell Carbon on Performance of Proton Exchange Membrane Fuel Cells. *J. Power Sources* **2009**, *193*, 17−23.
(41) Huang, H. J.; Wang, X. Design and Synthesis of Pd-MnO_2 Nanolamella-Graphene Composite as a High-Performance Multifunctional Electrocatalyst towards Formic Acid and Methanol Oxidation. *Phys. Chem. Chem. Phys.* **2013**, *15*, 10367−10375.
(42) Gao, H. L.; Liao, S. J.; Liang, Z. X.; Liang, H. G.; Luo, F. Anodic Oxidation of Ethanol on Core-Shell Structured Ru@PtPd/C Catalyst in Alkaline Media. *J. Power Sources* **2011**, *196*, 6138−6143.
(43) Wang, S. Y.; Yang, F.; Jiang, S. P.; Chen, S. L.; Wang, X. Tuning the Electrocatalytic Activity of Pt Nanoparticles on Carbon Nanotubes via Surface Functionalization. *Electrochem. Commun.* **2010**, *12*, 1646−1649.
(44) Ye, W. C.; Kou, H. H.; Liu, Q. Z.; Yan, J. F.; Zhou, F.; Wang, C. M. Electrochemical Deposition of Au-Pt Alloy Particles with Cauliflower-Like Microstructures for Electrocatalytic Methanol Oxidation. *Int. J. Hydrogen Energy* **2012**, *37*, 4088−4097.
(45) Xu, C. X.; Wang, L.; Mu, X. L.; Ding, Y. Nanoporous PtRu Alloys for Electrocatalysis. *Langmuir* **2010**, *26*, 7437−7443.
(46) Maiyalagan, T.; Scott, K. Performance of Carbon Nanofiber Supported Pd-Ni Catalysts for Electro-Oxidation of Ethanol in Alkaline Medium. *J. Power Sources* **2010**, *195*, 5246−5251.
(47) Ma, L.; Chu, D.; Chen, R. R. Comparison of Ethanol Electro-Oxidation on Pt/C and Pd/C Catalysts in Alkaline Media. *Int. J. Hydrogen Energy* **2012**, *37*, 11185−11194.
(48) Zhu, C. Z.; Guo, S. J.; Dong, S. J. PdM (M = Pt, Au) Bimetallic Alloy Nanowires with Enhanced Electrocatalytic Activity for Electro-Oxidation of Small Molecules. *Adv. Mater.* **2012**, *24*, 2326−2331.
(49) Huang, Z. Y.; Zhou, H. H.; Sun, F. F.; Fu, C. P.; Zeng, F. Y.; Li, T. Q.; Kuang, Y. F. Facile Self-Assembly Synthesis of PdPt Bimetallic Nanotubes with Good Performance for Ethanol Oxidation in an Alkaline Medium. *Chem.—Eur. J.* **2013**, *19*, 13720−13725.
(50) Hammer, B.; Nørskov, J. K. Theoretical Surface Science and Catalysis—Calculations and Concepts. *Adv. Catal.* **2000**, *45*, 71−129.
(51) Ruban, A.; Hammer, B.; Stoltze, P.; Skriver, H. L.; Nørskov, J. K. Surface Electronic Structure and Reactivity of Transition and Noble Metals. *J. Mol. Catal. A: Chem.* **1997**, *115*, 421−429.
(52) Nguyen, S. T.; Lawa, H. M.; Nguyena, H. T.; Kristiana, N.; Wang, S. Y.; Chan, S. H.; Wang, X. Enhancement Effect of Ag for Pd/C towards the Ethanol Electro-Oxidation in Alkaline Media. *Appl. Catal., B* **2009**, *91*, 507−515.
(53) Guo, S. J.; Dong, S. J.; Wang, E. K. Pt/Pd Bimetallic Nanotubes with Petal-Like Surfaces for Enhanced Catalytic Activity and Stability towards Ethanol Electrooxidation. *Energy Environ. Sci.* **2010**, *3*, 1307−1310.
(54) Zhu, C. Z.; Guo, S. J.; Dong, S. J. Facile Synthesis of Trimetallic AuPtPd Alloy Nanowires and Their Catalysis for Ethanol Electrooxidation. *J. Mater. Chem.* **2012**, *22*, 14851−14855.
(55) Chen, X. M.; Cai, Z. X.; Chen, X.; Oyamac, M. Green Synthesis of Graphene-PtPd Alloy Nanoparticles with High Electrocatalytic Performance for Ethanol Oxidation. *J. Mater. Chem. A* **2014**, *2*, 315−320.
(56) Lu, Y. Z.; Jiang, Y. Y.; Wu, H. B.; Chen, W. Nano-PtPd Cubes on Graphene Exhibit Enhanced Activity and Durability in Methanol Electrooxidation After CO Stripping−Cleaning. *J. Phys. Chem. C* **2013**, *117*, 2926−2938.
(57) Xu, C. W.; Shen, P. K.; Liu, Y. L. Ethanol Electrooxidation on Pt/C and Pd/C Catalysts Promoted with Oxide. *J. Power Sources* **2007**, *164*, 527−531.
(58) Chen, J. H.; Wang, M. Y.; Liu, B.; Fan, Z.; Cui, K. Z.; Kuang, Y. Platinum Catalysts Prepared with Functional Carbon Nanotube Defects and Its Improved Catalytic Performance for Methanol Oxidation. *J. Phys. Chem. B* **2006**, *110*, 11775−11779.